Theor Chem Acc (2003) 110: 421–427
DOI 10.1007/s00214-003-0497-4

Theoretical
Chemistry Accounts

Regular article

The maximum hardness and minimum polarizability principles as the basis for the study of reaction profiles

B. Gómez[1], **P. Fuentealba**[1], **R. Contreras**[2]

[1] Departamento de Física, Facultad de Ciencias, Universidad de Chile, Casilla 653 Santiago, Chile
[2] Departamento de Química, Facultad de Ciencias, Universidad de Chile, Casilla 653 Santiago, Chile

Received: 3 September 2002 / Accepted: 15 May 2003 / Published online: 25 November 2003

Abstract. New and useful aspects of chemical reactivity as described by reactivity indexes and used in connection with the maximum hardness and minimum polarizability principles (MHP and MPP, respectively) are discussed and illustrated for two classical reactions in organic chemistry. They include the Beckmann rearrangement and the condensation reactions of α-amino acids. The MPP appears as a more general rule than the MHP. Another relevant result is related to the usefulness of both empirical reactivity rules to predict the most probable reaction mechanism among two different pathways displaying very close values in activation energy (competitive pathways). This is illustrated for the condensation reaction of a series of α-amino acids: while the accepted stepwise route follows both the MHP and MPP rules, the alternative concerted channel does not, yet its associated activation energy is slightly lower than that corresponding to the nonconcerted reaction mechanism.

Keywords: Chemical reactivity – Maximum hardness principle – Minimum polarizability principle – Reaction mechanism

Introduction

In organic chemistry, there are a wide variety of reactions that are used as model systems in synthesis and for the identification of functional groups. Their classification in terms of reactivity and selectivity provides useful clues for possible synthetic routes and also to determine the main products of kinetic control expected for a given reaction, depending on field effects induced, for instance, by chemical substitution, solvent effects or other external sources in the environment. The change of a given reaction pattern naturally appears as a response to structural or environmental modifications, thereby allowing the treatment of chemical reactivity and selectivity in terms of global and local response functions. The static response functions defined in the context of density functional theory are conveniently represented as a derivative of the electronic energy, E, and electron density, $\rho(\mathbf{r})$, for an N-electron system in the field of an external potential, $v(\mathbf{r})$, due to the compensating nuclear charges. For instance, the energy changes induced by changes in N at constant $v(\mathbf{r})$ are described by the electronic chemical potential [1] defined by

$$\mu = \left(\frac{\partial E}{\partial N}\right)_{v(r)} \approx -\left(\frac{I+A}{2}\right) \approx \left(\frac{\varepsilon_H + \varepsilon_L}{2}\right). \quad (1)$$

This quantity may be estimated from the values of the vertical ionization potential, I, and the electron affinity, A, by a finite-difference formula [1]. In the absence of experimental data for I and A, it is still possible to get a reliable estimation of μ, using Koopmans' theorem, in terms of the one-electron energies of the HOMO (H) and LUMO (L) frontier molecular orbitals, as described in Eq. (1). The electronic chemical potential is the negative of the electronegativity [1] within this model, and it is the natural descriptor of charge transfer: while its absolute value is related to the amount of charge transfer, its sign describes the direction of the electron flux. During a molecular interaction, the electronic charge flux takes place from the molecular region presenting the highest values in μ towards the molecular region of lowest values of μ, until an equilibrium regime, where the electronic chemical potential acquires a uniform (equilibrium) value [1, 2].

The first derivative of the electronic chemical potential with respect to N at constant $v(\mathbf{r})$ provides a quantitative representation of Pearson's concept of

From the Proceedings of the 28th Congresco de Quimicos Teóricos de Expresión Latina (QUITEL 2002)

Correspondence to: P. Fuentealba
e-mail: p.fuentea@uchile.cl

chemical hardness [3]. The chemical hardness is a measure of the energy gap between the highest occupied and lowest virtual monoelectronic states in a molecule. Hard species interact favorably with other hard species (HSAB rule [4]). Hard species on the other hand, normally establish electrostatic interactions with a low charge transfer pattern. One of the most useful applications of the concept of chemical hardness has been consolidated in the form of an empirical rule (the maximum hardness principle MHP), stating that at constant electronic chemical potential, the natural evolution of molecular systems is towards a minimum energy value with a simultaneous increase in the chemical hardness [4]. Chemical hardness has a quantitative operational expression in terms of the I and A quantities, and also in terms of the one-electron molecular energy levels ε_H and ε_L, namely [1, 4]

$$\eta = \left(\frac{\partial \mu}{\partial N}\right)_{v(r)} \approx \left(\frac{I-A}{2}\right) = \left(\frac{\varepsilon_H - \varepsilon_L}{2}\right). \quad (2)$$

The inverse of the chemical hardness is the global softness [1, 4] $S = 1/\eta$, a quantity measuring the electronic polarizability of molecules [5], that conveniently complements the HSAB rule for hard species: the interaction between soft species is thermodynamically favorable with respect to the cross (hard/soft) interactions. Based on the relationship between global softness and the dipole polarizability [5], Chattaraj and Sengupta [6] proposed the minimum polarizability principle (MPP), which states that the natural evolution of molecular systems is towards a state of minimum polarizability. Therefore, while the softness profile is expected to parallel the energy profile during a chemical transformation, the hardness profile is expected to mirror both the energy and polarizability profiles.

Beside the global reactivity indexes, it is possible to define local response functions. For instance, the derivative of the electronic chemical potential with respect to the external potential defines the Fukui function $f(\mathbf{r})$ of the system [1]. The derivative of the electron density with respect to the electronic chemical potential defines the local softness, $s(\mathbf{r})$. Both quantities have been described as local reactivity indexes that determine selectivity [7, 8] in a molecule. Both quantities are related by $s(\mathbf{r}) = f(\mathbf{r})S$, thereby showing that the Fukui function acts as a distribution function for the global properties (S in the present case). There exist several definitions allowing local or regional Fukui functions for electrophilic, nucleophilic or radical attacks [9, 10, 11, 12] to be described, so that at present it is possible to conveniently characterize hard and soft electrophiles and nucleophiles, both globally and locally [12, 13, 14, 15]. Another pertinent aspect of local reactivity is related to the activation of sites in a molecule. Activation may be quantitatively represented as the variations in the local reactivity pattern at a given site, with reference to a slightly distorted structure or more correctly defined with reference to the transition state separating reactants and products. Consider, for instance, the variations in local softness [16, 17]:

$$\Delta s_k^\alpha = f_k^\alpha \Delta S^* + S \Delta f_k^\alpha, \quad (3)$$

where $\alpha = +$, $-$ or 0 for nucleophilic, electrophilic and radical attacks, respectively. The activation softness $\Delta S^* = S^{\#} - S^0$ is the difference in global softness for the system in the transition and ground states, and $\Delta f_k^\alpha = f_k^{\alpha,\#} - f_k^{\alpha,0}$ is the difference in the Fukui function at site k for the system in the transition and ground states. Note that Eq. (3) permits the calculation of activation softness at a given site, in terms of a global activation contribution driven by the first term, and a local activation contribution described by the second term of Eq. (3).

In this work we intend to illustrate how these electronic reactivity indexes may be used in connection with the empirical reactivity rules, to assist in the analysis of chemical reactivity, specifically those aspects related to the reaction mechanism. In order to evaluate these rules along a reaction profile, we selected the well-documented Beckmann rearrangement of oximes to yield the corresponding amides as products of the reaction. This reaction involves a series of intermediates and transition-state structures which will be used to evaluate both the MHP and MPP rules along a reaction profile. The second example involves the condensation reaction of α-amino acids. In this case, we show that both the MHP and the MPP rules may help to discriminate two competitive reaction mechanisms differing by a small amount in activation energy.

Computational details

Ground-state and transition-state structures were optimized at the B3LYP/6-311++G** level of theory. The calculation of chemical hardness using Eq. (2) was performed at the same level of theory within the Koopmans' theorem approximation. The dipole polarizability was evaluated as the mean value of the trace of the dipole polarizability tensor, namely,

$$<\alpha> = \frac{1}{3}(\alpha_{XX} + \alpha_{YY} + \alpha_{ZZ}), \quad (4)$$

using the GAUSSIAN98 suite of programs [18].

Results and discussion

Beckmann rearrangement

Aldoximes or ketoximes in the presence of Brönsted or Lewis acids readily rearrange into amides according to the reaction shown in Scheme 1. This intramolecular interconversion is known as the Beckmann rearrangement [19, 20, 21]. The reaction mechanism involves several intermediate species and transition-state structures. The Beckmann rearrangement of formaldehyde oxime (**1d**) is depicted in Scheme 2. The rearrangement initiates with the protonation of **1d** to yield methylene

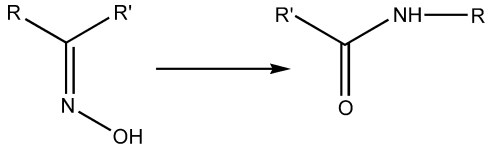

Scheme 1. Beckmann rearrangement

oxonium ion (**2a**). This species rearranges into **2b** by intramolecular proton transfer from the nitrogen atom to the oxygen site. The pathway from **2b** to **2c** is the Beckmann rearrangement itself, and the intermediate **2c** is known as the Beckmann product. This intermediate is unstable and may undergo nucleophilic attack by, for instance, an OH^- ion to yield formimidic acid (**3**). The final product, formamide (**4**), is obtained after a keto–enol tautomerization of **3**.

In this section we discuss the energy, hardness and polarizability profiles for the whole process shown in Scheme 2. It includes the formation of the formaldehyde oxime from the reaction of formaldehyde and hydroxilamine (steps **1a** + **1b** → **1d**). These steps involve two transition-state structures (**TS1** and **TS2** in Scheme 2) and one intermediate (**1c** in Scheme 2). Next we include the analysis of the second step from the formaldehyde oxime to the Beckmann product (**2a** → **2c**). This step involves two transition-state structures (**TS3** and **TS4** in Scheme 2) and one intermediate (**2b**) species. The third step, from **2c** to **3**, is a barrierless process. The fourth step is the tautomerization reaction of **3** to yield the final product **4**. This last step involves one additional transition state (**TS5**).

The energy profile for the first step (**1a** + **1b** → **1d**) is shown in Fig. 1. The activation energies for the formation of intermediates **1c** and **1d** are 30.2 and 43.5 kcal/mol, respectively, thereby showing that the elimination of water is the rate-determining step for this process, in which a carbon–oxygen bond is broken (Fig. 1). The first transition-state structure (**TS1**) has a unique

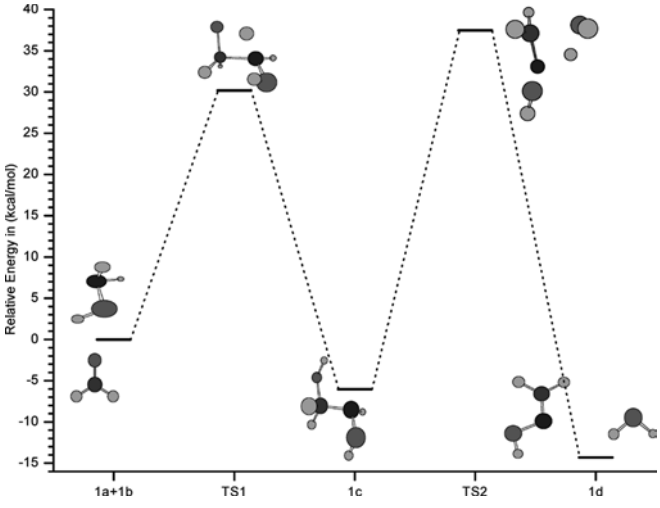

Fig. 1. Energy profile for the formation of formaldehyde oxime

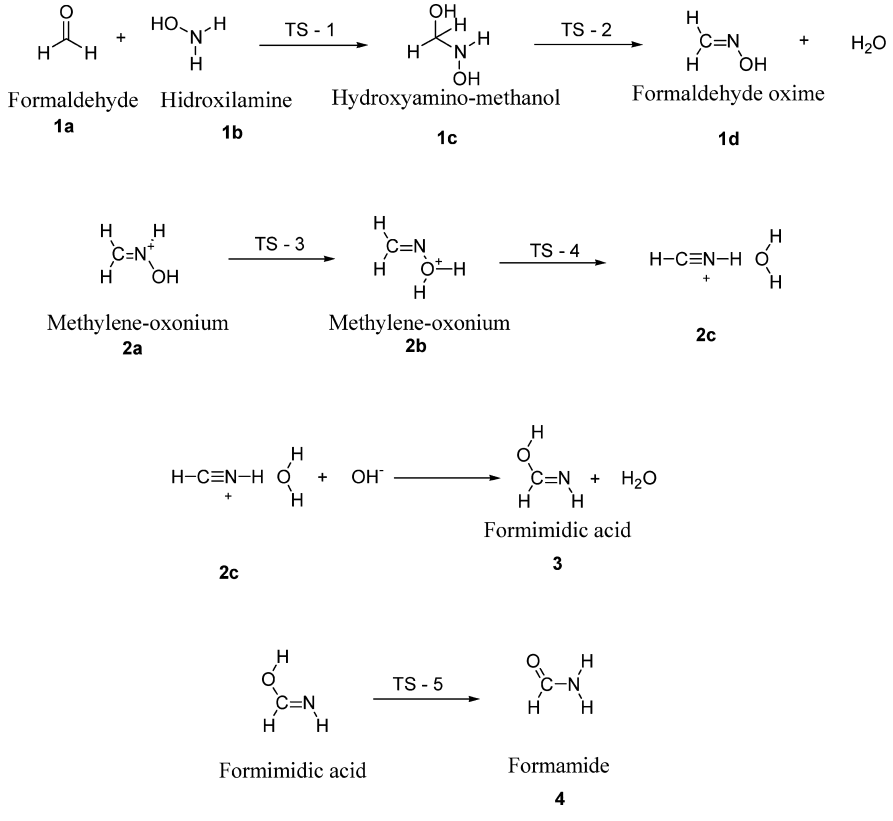

Scheme 2. Formation of formaldehyde oxime and reaction mechanism for the Beckmann transformation to formamide

Table 1. Total energy, chemical hardness and polarizability values for the formation of formaldehyde oxime. All values are in atomic units

Species	Energy	η	α
1a + **1b**	−246.2419	0.1305	41.16
TS1	−246.1938	0.1016	50.79
1c	−246.2515	0.1227	43.46
TS2	−246.1822	0.1027	59.25
1d + water	−246.2647	0.1300	45.64

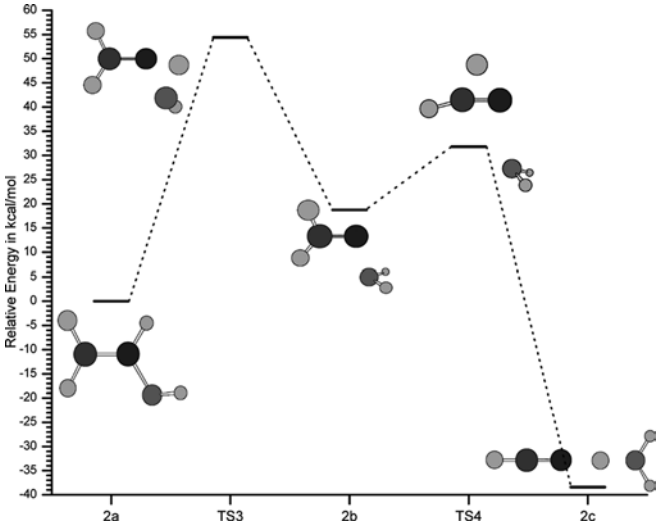

Fig. 2. Energy profile for the formation of the Beckmann product

imaginary frequency of 1,459.6*i* associated with the stretching mode between the carbon and nitrogen atoms. The second transition state (**TS2**) has a unique imaginary frequency of 1,957.6*i*, associated with the water elimination. The energy, hardness and polarizability results for this step are summarized in Table 1. It may be seen that the MHP is fulfilled for the step **1a** + **1b** → **1d**: ground and intermediate states have hardness values greater than those associated with the transition-state structures (**TS1** and **TS2**). Note also that the ground and intermediate states have polarizability values lower than those associated with transition-state structures **TS1** and **TS2**.

The energy profile for the second step (**2a** → **2c**) is summarized in Fig. 2. There are two transition-state structures associated with this step. The first one, **TS3**, is characterized by a unique imaginary frequency of 1,862.2*i* associated with the proton migration from the nitrogen to the oxygen atom, which concertedly occurs with the increase in the nitrogen–oxygen distance. The second transition state structure for this step, **TS4**, is characterized by a unique imaginary frequency of 788.9*i*, corresponding to Beckmann rearrangement itself (i.e., the migration of a hydrogen atom from the carbon to the nitrogen atom). The energy, hardness and polarizability results for this step are summarized in Table 2. It may be seen that

Table 2. Energy, chemical hardness, polarizability values and harmonic vibrational analysis for the formation of the Beckmann product. All values are in atomic units

Species	Energy	η	α	Number of imaginary frequencies	Frequency
2a	−170.1315	0.1233	32.36	0	
TS3	−170.0448	0.1401	36.88	1	1,862.2*i*
2b	−170.1016	0.1365	35.66	0	
TS4	−170.0808	0.0936	39.41	1	788.9*i*
2c	−170.1927	0.1897	28.19	0	

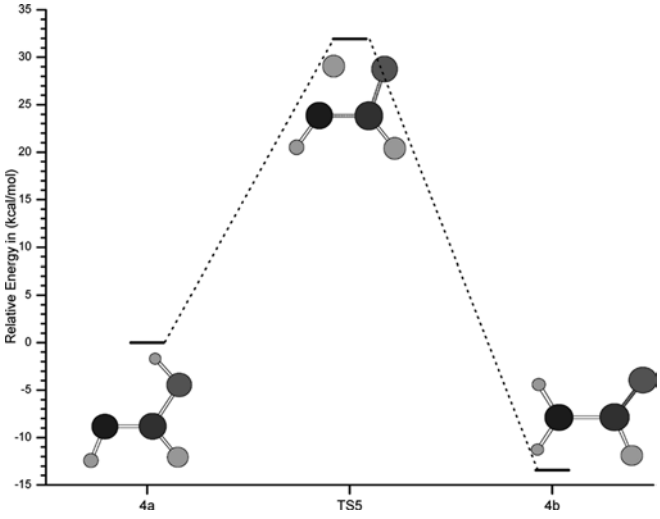

Fig. 3. Energy profile for the **3** → **4** tautomerization

while the MPP rule is satisfactory fulfilled, the MHP rule is not. The ground and intermediate states have polarizability values that are lower than transition-state structures **TS3** and **TS4**, the **TS3** structure is harder than the intermediate **2b** but softer than the Beckmann product **2c**.

The energy profile for the tautomerization step leading to formamide, the final product of the reaction, is shown in Fig. 3. The tautomerization reaction is characterized by an activation energy of 32.0 kcal/mol. The transition-state structure **TS5** has a unique imaginary frequency of 1,952.9*i* (Table 3). Here again the MPP rule is satisfactorily fulfilled but the MHP is violated: transition state **TS5** is softer than tautomer **3** but harder than the ground-state product **4**.

Beside the global reactivity analysis performed on the basis of the total energy, the chemical hardness and the dipole polarizability of the species involved in the Beckmann rearrangement of formaldehyde oxime to formamide, a local analysis was also performed. This analysis was made on the basis of the Fukui function. For instance, for the first step, formaldehyde has the highest value of the electrophilic Fukui function (i.e., the Fukui function for nucleophilic attack $f^{+} = 0.72$) at

Table 3. Energy, chemical hardness, polarizability values and harmonic vibrational analysis for the **3** → **4** tautomerization. All values are in atomic units

Species	Energy	η	α	Number of imaginary frequencies	Frequency
3	−169.8882	0.1441	35.53	0	
TS5	−169.8373	0.1296	38.75	1	1,952.9*i*
4	−169.9009	0.1273	34.88	0	

the carbon atom. This is the active center for the nucleophilic attack by hydroxylamine. This result also coincides with the local reactivity picture developed in hydroxylamine: the highest value of the nucleophilic Fukui function is found at the nitrogen center ($f^- = 0.73$). Both results are also consistent with the population analysis performed using the atomic charges derived from the electrostatic potential. For the intermediate steps, however, the Fukui function formalism is not sufficient to correctly assess the local reactivity patterns of the intermediates. However, in these cases a more complete picture may be obtained by looking at the variations in local softness with reference to the corresponding transition-state structures (activation softness), given by Eq. (3). This quantity encompasses both the local activation driven by the variations in the Fukui function and also the variation in global softness from the ground-state to the transition-state structures. For instance, in the second step (**2a** → **2c**), leading to the Beckmann product, the highest activation softness, Δs_k^+, with reference to the **TS4** structure for electrophilic attack is consistently found at the carbon atom of structure **2b**.

Condensation reaction of α-amino acids

In the preceding section we analyzed the Beckmann rearrangement to illustrate how the MPP and MHP rules may be used as complementary tools to study the relative stability of species involved in a complex reaction path involving a high number of intermediates and transition-state structures. The local analysis correctly complements the information obtained from the global and energy analysis of the reaction profile. In this section we show the practical utility of the MHP and MPP rules to elucidate the most probable reaction mechanism for a chemical process that presents two competitive pathways (i.e. two different reaction paths differing by a small amount in activation energy). The analysis is performed on the condensation reaction of a series of α-amino acids. The accepted reaction mechanism is illustrated for glycine in Scheme 3. It suggests that the reaction proceeds within a stepwise reaction channel where the nucleophilic attack of the amino group on the carbonylic carbon center leads to the formation of a geminal diol intermediate (Scheme 3). This step involves transition-state **TS6**. The condensation product is attained after water elimination that involves a second transition-state structure, **TS7**. The predicted activation energy for the rate-determining step (i.e., the formation of the geminal diol intermediate) is predicted to be 40.2, 41.7, 42.6 and 43.4 kcal/mol for the reaction of glycine with glycine, alanine, isoleucine and leucine, respectively.

A second concerted reaction mechanism may be proposed. This reaction mechanism is depicted in Scheme 4. It involves a unique transition-state structure, **TS8**. The corresponding activation energies are 39.7, 38.7, 41.4 and 41.2 kcal/mol, for the same reactions of

Table 4. Energy, chemical hardness, global softness, polarizability values and harmonic vibrational analysis for the stepwise condensation of α-amino acids. All values are in atomic units, except ΔE, which is given in kilocalories per mole

Species		Energy	η	S	α	Number of imaginary frequencies	Frequency	ΔE
Glycine	Reactants	−568.72	3.49	0.29	94.78	0		0.0
	TS6	−568.65	2.77	0.36	100.86	1	1,551.6*i*	40.2
	Geminal diol intermediate	−568.7	2.98	0.34	96.01	0		8.9
	TS7	−568.66	2.84	0.35	103.82	1	1,565.8*i*	35.9
	Products	−568.71	3.09	0.32	96.76	0		5.5
Alanine	Reactants	−608.01	3.45	0.29	109.44	0		0.0
	TS 6	−607.94	2.73	0.37	116.23	1	1,576.4*i*	41.7
	Geminal diol intermediate	−607.99	2.93	0.34	110.87	0		9.0
	TS 7	−607.95	2.81	0.36	118.70	1	1,561.7*i*	35.5
	Products	−608	3.09	0.32	111.90	0		5.7
Isoleucine	Reactants	−725.87	3.38	0.3	153.71	0		0.0
	TS6	−725.8	2.72	0.37	160.28	1	1,585.7*i*	42.6
	Geminal diol intermediate	−725.85	2.91	0.34	154.90	0		11.5
	TS7	−725.81	2.81	0.36	162.99	1	1,540.1*i*	35.3
	Products	−725.86	3.06	0.33	156.07	0		4.6
Leucine	Reactants	−725.87	3.4	0.29	153.73	0		0.0
	TS6	−725.8	2.72	0.37	160.41	1	1,588.2*i*	43.4
	Geminal diol intermediate	−725.85	2.92	0.34	155.12	0		10.3
	TS7	−725.81	2.81	0.36	163.35	1	1,539.2*i*	36.8
	Products	−725.86	2.95	0.34	156.58	0		4.0

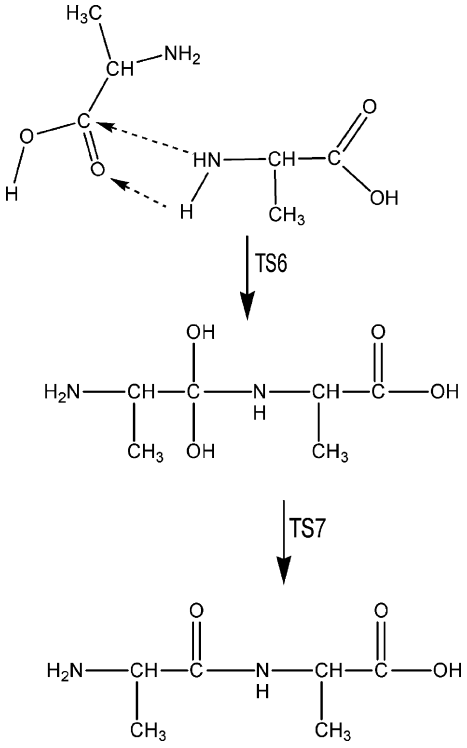

Scheme 3. Reaction mechanism for the stepwise condensation of glycine

glycine with glycine, alanine, isoleucine and leucine, respectively. Note that the proposed concerted mechanism has activation energy values even lower than those associated with the accepted mechanism. The complete global and energy analyses are summarized in Tables 4 and 5 for both possible mechanisms. From Table 4, it may be seen that both the MPP and MHP are satisfactorily fulfilled for the accepted stepwise reaction mechanism. However, for the proposed concerted reaction channel, while the MPP rule is satisfied for the whole series of reactions, the MHP systematically fails. This result is interesting in the sense that the empirical MHP and MPP rules can be used as complementary tools to assist in the characterization of reaction mechanisms in those processes presenting very close values in activation

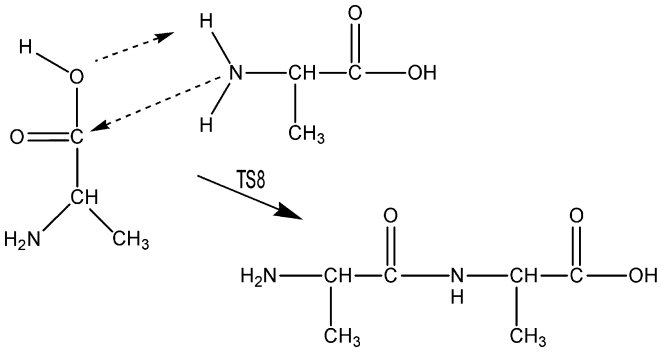

Scheme 4. Reaction mechanism for the concerted condensation of glycine

energy. Therefore, as it was previously demonstrated that both empirical reactivity rules consistently complemented the Woodward–Hoffmann symmetry rules [22], it seems that the most probable reaction mechanisms are also expected to simultaneously follow both empirical principles of reactivity.

Concluding remarks

The MHP and the MPP for two classical reactions in organic chemistry have been examined. While the MPP rule is satisfactorily fulfilled along the complete reaction profile, the MHP is not. The relationship between energy and hardness fails when comparisons between transition-state structures, intermediates and ground states are made. The effect of the whole set of molecular orbitals for the calculation of dipole polarizability may have some influence on this result, as the operational chemical hardness is only related to the energy gap between the frontier molecular orbitals. Hence, those reactions which are not driven by the HOMO/LUMO states are not expected to follow the MHP. Both MHP and MPP empirical rules have been used to study the reaction profile of two competitive mechanisms differing by a small amount in activation energy. While the experimentally accepted reaction mechanism has an energy profile which is consistent with both reactivity

Table 5. Energy, chemical hardness, global softness, polarizability values and harmonic vibrational analysis for the concerted condensation of α-amino acids. All values in atomic units, except ΔE, which is given in kilo calories per mole

Species		Energy	η	S	α	Number of imaginary frequencies	Frequency	ΔE
Glycine	Reactants	−568.7164	3.49	0.29	94.78	0		0.0
	TS8	−568.6530	3.11	0.32	105.95	1	1,291.9*i*	39.7
	Products	−568.7077	3.09	0.32	96.76	0		5.5
Alanine	Reactants	−608.0071	3.45	0.29	109.44	0		0.0
	TS8	−607.9454	3.1	0.32	121.17	1	1,260.9*i*	38.7
	Products	−607.9980	3.09	0.32	111.90	0		5.7
Isoleucine	Reactants	−725.8677	3.38	0.3	153.71	0		0.0
	TS8	−725.8017	3.11	0.32	166.33	1	1,231.8*i*	41.4
	Products	−725.8603	3.06	0.33	156.07	0		4.6
Leucine	Reactants	−725.8696	3.4	0.29	153.73	0		0.0
	TS8	−725.8040	3.11	0.32	165.93	1	1,221.2*i*	41.2
	Products	−725.8633	2.95	0.34	156.58	0		4.0

principles, the energy profile of the proposed reaction mechanism follows the MPP rule but the MHP rule consistently fails.

Acknowledgements. This work received financial support from Fondecyt, grants 2000092, 1010649 and 1030548. B.G. is a DAAD fellow.

References

1. Parr RG, Yang W (1989) Density functional theory of atoms and molecules. Oxford University Press, New York
2. (a) Hohenberg P, Kohn W (1964) Phys Rev B 136:864; (b) Milleken RS (1934) J Chem Phys 2:782; (c) Parr RG, Donelly RA, Levy M, Palke WE (1978) J Chem Phys 68:3801; (d) Sen KD, Joergensen CK (1987) Electronegativity. Springer, Berlin Heidelberg New York
3. Parr RG, Pearson RG (1983) J Am Chem Soc 105:7512
4. (a) Pearson RG (1973) Hard and soft acids and bases. Dowden, Hutchinson and Ross, Stroudsberg, PA; (b) Pearson RG (1963) J Am Chem Soc 85:3533
5. Fuentealba P, Simon-Manso Y, Chattaraj PK (2000) J Phys Chem A 104:3185
6. Chattaraj PK, Sengupta S (1996) J Phys Chem 100:16126
7. Li Y, Evans JNS (1995) J Am Chem Soc 117:7756
8. Pérez P, Simón-Manso Y, Aizman A, Fuentealba P, Contreras R (2000) J Am Chem Soc 122:4756
9. Yang W, Mortier W (1986) J Am Chem Soc 108:5708
10. Contreras R, Fuentealba P, Galván M, Pérez P (1999) Chem Phys Lett 304:405
11. Fuentealba P, Pérez P, Contreras R (2000) J Chem Phys 113:2544
12. Santos JC, Contreras R, Chamorro E, Fuentealba P (2001) J Chem Phys 116:4311
13. Pérez P, Toro-Labbé A, Contreras R (2001) J Am Chem Soc 123:5527
14. Pérez P, Aizman A, Contreras R (2002) J Phys Chem A 106:3964
15. Domingo LR, Aurrell MJ, Pérez P, Contreras R (2002) Tetrahedron 58:4417
16. Contreras R, Domingo LR, Andrés J, Pérez P, Tapia O (1999) J Phys Chem A 103:1367
17. Aizman A, Contreras R, Galván M, Cedillo E, Chamorro E, Santos JC (2002) J Phys Chem A
18. Frisch MJ, Trucks GW, Schlegel HB, Scuseria GE, Robb MA, Cheeseman JR, Zakrzewski VG, Montgomery JA Jr, Stratmann RE, Burant JC, Dapprich S, Millam JM, Daniels AD, Kudin KN, Strain MC, Farkas O, Tomasi J, Barone V, Cossi M, Cammi R, Mennucci B, Pomelli C, Adamo C, Clifford S, Ochterski J, Petersson GA, Ayala PY, Cui Q, Morokuma K, Malick DK, Rabuck AD, Raghavachari K, Foresman JB, Cioslowski J, Ortiz JV, Baboul AG, Stefanov BB, Liu G, Liashenko A, Piskorz P, Komaromi I, Gomperts R, Martin RL, Fox DJ, Keith T, Al-Laham MA, Peng CY, Nanayakkara A, Challacombe M, Gill PMW, Johnson B, Chen W, Wong MW, Andres JL, Gonzalez C, Head-Gordon M, Replogle ES, Pople JA (1998) Gaussian 98, revision A.9. Gaussian, Pittsburgh, PA
19. Beckmann E (1886) Chem Ber 89:988
20. (a) March J (1996) Advanced organic Chemistry, 3rd edn. McGraw-Hill, New York, p 942; (b) Nguyen T, Vanquickenborne LG (1993) J Chem Soc Perkin Trans 2 1969; (c) Carey FA, Sundberg RJ (1990) Advanced organic chemistry, 3rd edn. Plenum, New York, p 540
21. (a) Hendrickson, JB, Cram DJ, Hammond GS (1970) organic chemistry 3rd edn. McGraw-Hill, New York, p 708; (b) Blatt AH (1933) Chem Rev 12:215; (c) Jones B (1944) Chem Rev 35:335; (d) Moller F (1957) In: Müller E (ed) Methoden der Organischem Chemie vol 11, part 1. Thieme, Stuttgart, p 892; (e) Donaruma LG, Heldt WZ (1960) Org React 1:11; (f) Berckwith ALJ (1970) In: Zabicky J (ed) The chemistry of amides. Interscience, New York, p 131; (g) McCarty CG (1970) In: Patai S (ed) The chemistry of the carbon–nitrogen double bond. Interscience, New York, p 408; (h) Smith PAS (1963) In: De Mayo P (ed) Molecular rearrangements. Interscience, New York, p 45; (i) Mukamal H (1971) Nuova Chim 47:79; (j) Hornke G, Krauch H, Kunz W (1965) Chem Zgt 89:525; (k) Gawley RE (1988) Org React 35:1; (l) Jochims JC, Hehl S, Herzberger S (1990) Synthesis 1128; (m) Hesse M (1991) Ring enlargement in Organic Chemistry. VCH, Weinheim
22. Chattaraj PK, Fuentealba P, Badhin Gómez, Contreras R (2000) J Am Chem Soc 122:348